

Testing lepton flavor universality in terms of BESIII and charm-tau factory data^{*}

WANG Bin(王彬)^{1;1)} ZHAO Ming-Gang(赵明刚)^{1;2)} SUN Ke-Sheng(孙科盛)^{2,3;3)}
LI Xue-Qian(李学潜)^{1;4)}

¹ School of Physics, Nankai University, Tianjin 300071, China

² Department of Physics, Dalian University of Technology, Dalian 116024 China

³ School of Physics, Hebei University, Baoding 071002, China

Abstract: The recent measurements on R_K and R_π imply that there exists a possible violation of the leptonic flavor universality which is one of the cornerstones of the Standard Model. It is suggested that a mixing between sterile and active neutrinos might induce such a violation. In this work we consider the scenarios with one or two sterile neutrinos to explicitly realize the data while the constraints from the available experiments have been taken into account. Moreover, as indicated in literature, the deviation of the real PMNS matrix from the symmetric patterns may be due to a μ - τ asymmetry, therefore the measurements on $R_{D(D_s)e\mu} = \Gamma(D(D_s) \rightarrow e^+\nu_e)/\Gamma(D(D_s) \rightarrow \mu^+\nu_\mu)$ and $R_{D(D_s)\mu\tau} = \Gamma(D(D_s) \rightarrow \mu^+\nu_\mu)/\Gamma(D(D_s) \rightarrow \tau^+\nu_\tau)$ (and for some other heavy mesons B^\pm and B_c etc.) may shed more light on the physics responsible for the violation of the leptonic flavor universality. The data of BESIII are available to test the universality and that of future charm-tau factories will provide more accurate information. In this work, we will discuss $R_{D(D_s)e\mu}$ and $R_{D(D_s)\mu\tau}$ in detail and also briefly consider the cases for B^\pm and B_c .

Key words: neutrino mass and mixing, lepton flavor universality, sterile neutrino

PACS: 14.60.Pq, 14.60.St, 13.20.Jf **DOI:** 10.1088/1674-1137/37/7/073101

1 Introduction

The property that couplings of leptons to gauge bosons are independent of lepton flavors is called lepton flavor universality (LFU), which is embedded in the Standard Model (SM) and any violation of LFU may be induced by new physics beyond the SM. Taking leptonic decays of W boson $W \rightarrow l\nu_l$ ($l=e, \mu, \tau$) as an instance, ratios of the branching fractions measured at LEP II [1] are

$$B(W \rightarrow \mu\bar{\nu}_\mu)/B(W \rightarrow e\bar{\nu}_e) = 0.997 \pm 0.021, \quad (1)$$

$$B(W \rightarrow \tau\bar{\nu}_\tau)/B(W \rightarrow e\bar{\nu}_e) = 1.058 \pm 0.029, \quad (2)$$

$$B(W \rightarrow \tau\bar{\nu}_\tau)/B(W \rightarrow \mu\bar{\nu}_\mu) = 1.061 \pm 0.028. \quad (3)$$

corresponding to 0.1σ , 2σ , and 2.2σ deviation from the SM predictions. The issue of τ lepton universality was

also discussed in Ref. [2] in the framework of effective field theory. Besides, leptonic decays of mesons also provide a possibility to test LFU where the uncertainties in the hadronic sector are cancelled. In literature the ratios are suggested to be measured

$$R_{P\alpha\beta} \equiv \frac{\Gamma(P^+ \rightarrow \alpha^+\nu_\alpha)}{\Gamma(P^+ \rightarrow \beta^+\nu_\beta)}, \quad (4)$$

where $P=\pi, K, D, D_s, B, B_c$ and $\alpha, \beta=e, \mu, \tau$. In order to clearly demonstrate deviation of the measured value $R_{P\alpha\beta}^{\text{exp}}$ from the SM predictions $R_{P\alpha\beta}^{\text{SM}}$, a parameter $\Delta r_{P\alpha\beta}$ is defined as

$$\Delta r_{P\alpha\beta} \equiv \frac{R_{P\alpha\beta}^{\text{exp}}}{R_{P\alpha\beta}^{\text{SM}}} - 1. \quad (5)$$

To accommodate non-zero $\Delta r_{P\alpha\beta}$, one may invoke two different mechanisms [3].

Received 7 April 2013

^{*} Supported by National Natural Science Foundation of China (11075079, 11135009)

1) E-mail: wangbin070068@mail.nankai.edu.cn

2) E-mail: zhaomg@nankai.edu.cn

3) E-mail: sunkesheng@126.com

4) E-mail: lixq@nankai.edu.cn

©2013 Chinese Physical Society and the Institute of High Energy Physics of the Chinese Academy of Sciences and the Institute of Modern Physics of the Chinese Academy of Sciences and IOP Publishing Ltd

1) Introducing a new Lorentz structure in the four-fermion interaction.

2) Modifying the $Wl\nu_1$ vertex by corrections to lepton mixing.

For the first category, the SM may be extended to new physics beyond the Standard Model (BSM) which includes charged Higgs, for example in the supersymmetry (SYSY) [4] or two-Higgs-doublet models [5]. In the SM, the violation of LFU is estimated as

$$|\Delta r_{P\alpha\beta}^{\text{SM}}| = \mathcal{O}\left(\frac{\alpha}{4\pi} \times \frac{m_{\alpha(\beta)}^2}{m_W^2}\right),$$

which is too small to be accounted for, while for the first category, the correction to the $W\alpha\nu_\alpha$ vertex emerges at the loop level where new physics BSM particles exist is of order

$$\mathcal{O}\left(\frac{\alpha}{4\pi} \times \frac{m_W^2}{\Lambda_{\text{NP}}^2}\right),$$

which is greatly suppressed by the new physics scale Λ_{NP} [6].

For the second category, the coupling $W\alpha\nu_\alpha$ is modified by breaking the unitarity of the 3×3 lepton mixing matrix. In the type-I seesaw [7], sterile neutrinos are introduced and the 3×3 mixing matrix could be non-unitary to the level of $\mathcal{O}(M_D^2/M_R^2)$ [8, 9], where M_D and M_R are the Dirac and Majorana mass matrices, respectively.

Introducing sterile neutrinos can provide natural interpretations of some anomalies observed in recent experiments. For instance, the LSND [10], the MiniBooNE [11], the reactor [12] anomalies and as well as the gallium anomaly of the GALLEX [13] and SAGE [14] experiments. Furthermore, a careful analysis of the cosmological data shows that the effective number of neutrino species is larger than 3 [15], which might also hint at the existence of an additional one or two neutrino species besides the three active ones. Therefore a study on violation of LFU would be interesting because it may reveal possible new physics mechanisms beyond the SM at the lepton sector.

As indicated in literature, the deviation of the real PMNS matrix from the symmetric patterns may be due to a μ - τ asymmetry. Kinematic constraints mean that K and π cannot decay into $\tau\nu$, so measurements on $R_{D(D_s)e\mu} = \Gamma(D(D_s) \rightarrow e^+\nu_e)/\Gamma(D(D_s) \rightarrow \mu^+\nu_\mu)$ and $R_{D(D_s)\mu\tau} = \Gamma(D(D_s) \rightarrow \mu^+\nu_\mu)/\Gamma(D(D_s) \rightarrow \mu^+\tau_\tau)$ (and some other heavy mesons B^\pm and B_c etc.) may shed more light on the physics responsible for the violation of the leptonic flavor universality. The data of BES III are available to test the universality and measurements at future charm-tau factories will provide more accurate information in this regard. Indeed, the experimental results of the NA62 Collaboration [16] determine $\Delta r_{K_{e\mu}} = (4 \pm 4) \times 10^{-3}$ and $\Delta r_{\pi_{e\mu}} = (-4 \pm 3) \times 10^{-3}$

[3] whereas the BES data tell us $\Delta r_{D_s\mu\tau} = 0.256_{-0.317}^{+0.430}$ which is rather large.

The presence of sterile neutrinos changes the leptonic decay widths of pseudoscalar mesons and then $\Delta r_{P\alpha\beta}$ may be enhanced or suppressed. In this work we start with this motivation and derive the analytical formulas of $\Delta r_{P\alpha\beta}$ for 3+1 and 3+2 scenarios in the next section. Especially in this work, we will discuss $R_{D(D_s)e\mu}$ and $R_{D(D_s)\mu\tau}$ in detail and also briefly consider the cases for B^\pm and B_c . Numerical analyses are made and possible experimental measurements on $\Delta r_{P\alpha\beta}$ at BES and future charm-tau factories are discussed. Then we present some discussions in the last section.

2 $R_{P\alpha\beta}$ within the SM

In the SM, the leptonic decay widths of pseudo-scalar mesons $P \rightarrow \alpha\nu_\alpha$ ($\alpha=e, \mu$ or τ and $P=\pi, K, D, D_s, B$ or B_c) are given by

$$\Gamma_{P \rightarrow \alpha\nu_\alpha}^{\text{SM}} = \frac{G_F^2}{8\pi} |V_{qq'}|^2 f_P^2 m_P m_\alpha^2 \left(1 - \frac{m_\alpha^2}{m_P^2}\right)^2, \quad (6)$$

where G_F is the Fermi constant, m_α is the lepton mass, $V_{qq'}$ the element of the Cabibbo-Kobayashi-Maskawa (CKM) mixing matrix corresponding to the constituents in the meson P whose mass is m_P and decay constant f_P and neutrino masses are neglected. As is well known, these processes are helicity suppressed.

With the definition of $\Gamma_{P \rightarrow \alpha\nu_\alpha}^{\text{SM}}$ in Eq. (6), one has

$$R_{P\alpha\beta}^{\text{SM}} \equiv \left(\frac{m_\alpha}{m_\beta}\right)^2 \left(\frac{m_P^2 - m_\alpha^2}{m_P^2 - m_\beta^2}\right)^2. \quad (7)$$

If the QED corrections are considered, there will be a factor $(1 + \delta_{\text{QED}})$ multiplying to the left-handed side of Eq. (7). An approximate estimate of electrodynamic correction to $P \rightarrow \alpha\nu_\alpha$ is about $\frac{1}{137} \times \frac{1}{2\pi} \sim 10^{-3}$ suppression. For the leptonic kaon decay, due to the inner bremsstrahlung $K_{l2\gamma}$ process which is included by definition into R_K , the calculation indicates $\delta_{\text{QED}} = (-3.78 \pm 0.04)\%$ [17].

As suggested, the existence of sterile neutrinos changes the picture, so in the next section, we will study how they contribute to $P \rightarrow \alpha\nu_\alpha$.

3 Lepton mixing with the presence of sterile neutrinos

Now let us give a general description of the involvement of sterile neutrinos and take 3+1 as an illustration. In the SM, the sterile neutrinos do not directly couple to W -bosons, thus without mixing between sterile neutrinos and active ones, the weak interaction can be written

as

$$\overline{(e, \mu, \tau)} \gamma^\mu (1 - \gamma_5) (U_{\text{PMNS}}, 0) \begin{pmatrix} \nu_1 \\ \nu_2 \\ \nu_3 \\ \nu_s \end{pmatrix} W_\mu, \quad (8)$$

where ν_i ($i=1, 2, 3$) are the active neutrinos and ν_s is a sterile neutrino (or several), U_{PMNS} is the regular PMNS lepton mixing matrix and here 0 denotes a 3×1 matrix, thus $(U_{\text{PMNS}}, 0)$ is a 3×4 matrix and in this scenario, unitarity no longer exists. When the mixing between ν_s and ν_i is introduced, the matrix becomes $(U_{\text{PMNS}} \cdot \cos \epsilon, \sin \epsilon)$ and the coupling vertex is

$$\overline{(e, \mu, \tau)} \gamma^\mu (1 - \gamma_5) (U_{\text{PMNS}} \cdot \cos \epsilon, \sin \epsilon) \begin{pmatrix} \nu_1 \\ \nu_2 \\ \nu_3 \\ \nu_s \end{pmatrix} W_\mu, \quad (9)$$

then the sterile neutrino participates in the weak interaction¹⁾. Meanwhile this mixing also induces a

$$\Gamma_{\text{P} \rightarrow \alpha \nu \alpha}^s = \frac{G_{\text{F}}^2}{8\pi} |V_{\text{PP}'}|^2 f_{\text{P}}^2 m_{\text{P}} \times \left[\sum_{i=1}^3 |U_{\alpha i}|^2 m_\alpha^2 \left(1 - \frac{m_\alpha^2}{m_{\text{P}}^2}\right)^2 + \sum_{i=1}^{N-3} |U_{\alpha, i+3}|^2 (m_\alpha^2 + m_{s_i}^2) \left(1 - \frac{m_\alpha^2 + m_{s_i}^2}{m_{\text{P}}^2}\right) \frac{\lambda(m_{\text{P}}^2, m_\alpha^2, m_{s_i}^2)}{m_{\text{P}}^2} \right], \quad (11)$$

where m_{s_i} is the sterile neutrino masses and N is the total number of neutrino mass eigenstates, for instance, assuming two sterile neutrinos, i.e., the so-called 3+2 scenario [18], $N=3+2=5$. The $\lambda(m_{\text{P}}^2, m_\alpha^2, m_{s_i}^2)$ is defined as

$$\lambda(m_{\text{P}}^2, m_\alpha^2, m_{s_i}^2) = \sqrt{m_{\text{P}}^4 + m_\alpha^4 + m_{s_i}^4 - 2m_{\text{P}}^2 m_\alpha^2 - 2m_{\text{P}}^2 m_{s_i}^2 - m_\alpha^2 m_{s_i}^2}. \quad (12)$$

Now we can obtain the general expression of $\Delta r_{\text{P}\alpha\beta}$

$$\Delta r_{\text{P}\alpha\beta} = \frac{R_{\text{P}\alpha\beta}^s}{R_{\text{P}\alpha\beta}^{\text{SM}}} - 1, \quad (13)$$

where $R_{\text{P}\alpha\beta}^{\text{SM}}$ is obtained in Eq. (7) and

$$R_{\text{P}\alpha\beta}^s = \frac{\sum_{i=1}^3 |U_{\alpha i}|^2 m_\alpha^2 (m_{\text{P}}^2 - m_\alpha^2)^2 + \sum_{i=1}^{N-3} |U_{\alpha, i+3}|^2 (m_\alpha^2 + m_{s_i}^2) (m_{\text{P}}^2 - m_\alpha^2 - m_{s_i}^2) \lambda(m_{\text{P}}^2, m_\alpha^2, m_{s_i}^2)}{\sum_{j=1}^3 |U_{\beta j}|^2 m_\beta^2 (m_{\text{P}}^2 - m_\beta^2)^2 + \sum_{j=1}^{N-3} |U_{\beta, j+3}|^2 (m_\beta^2 + m_{s_j}^2) (m_{\text{P}}^2 - m_\beta^2 - m_{s_j}^2) \lambda(m_{\text{P}}^2, m_\beta^2, m_{s_j}^2)}. \quad (14)$$

3.1 3+1 scenario

In order to get the 3×4 mixing matrix describing the sterile-active neutrino mixing in charged-current and neutral-current interactions, an easy means is to construct a 4×4 matrix in a regular way and then remove the last row of the 4×4 matrix to get the required 3×4 matrix. The 3×5 matrix for the 3+2 scenario will be obtained in a similar way.

First we deal with the case by adding one sterile neutrino into the game, i.e., the 3+1 scenario, in which the lepton mixing matrix can be parameterized with 6 mix-

ing angles and 3 phases in a form

$$\overline{(\nu_1, \nu_2, \nu_3, \nu_s)} \gamma^\mu (1 - \gamma_5) (1, 0) \begin{pmatrix} \nu_1 \\ \nu_2 \\ \nu_3 \\ \nu_s \end{pmatrix} \times Z_\mu \rightarrow \overline{(\nu_1, \nu_2, \nu_3, \nu_s)} \gamma^\mu (1 - \gamma_5) V' \begin{pmatrix} \nu_1 \\ \nu_2 \\ \nu_3 \\ \nu_s \end{pmatrix} Z_\mu, \quad (10)$$

where V' is a 4×4 matrix and results from a matrix product of $(4 \times 3) \otimes (3 \times 4)$, i.e., $(U_{\text{PMNS}} \cdot \cos \epsilon, \sin \epsilon)^\dagger (U_{\text{PMNS}} \cdot \cos \epsilon, \sin \epsilon)$. This non-unitary mixing matrix and sizable sterile neutrino masses can also change the generation number which is accurately measured by the LEP experiment. Therefore the mixing is rigorously constrained by the LEP data.

Once sterile neutrinos are introduced, they do indeed mix with active ones, the decay width obtained above (6) will be modified into

ing angles and 3 phases in a form

$$U_{3+1} = R_{34}(\theta_{34}, \delta_{34}) R_{24}(\theta_{24}, 0) R_{14}(\theta_{14}, \delta_{14}) R_{23}(\theta_{23}, 0) \times R_{13}(\theta_{13}, \delta_{13}) R_{12}(\theta_{12}, 0), \quad (15)$$

where R_{ij} is a 4×4 matrix describing the rotation in the i - j plane and here presents R_{34} as an instance,

$$R_{34}(\theta_{34}, \delta_{34}) = \begin{pmatrix} 1 & 0 & 0 & 0 \\ 0 & 1 & 0 & 0 \\ 0 & 0 & \cos \theta_{34} & \sin \theta_{34} e^{-i\delta_{34}} \\ 0 & 0 & -\sin \theta_{34} e^{i\delta_{34}} & \cos \theta_{34} \end{pmatrix}. \quad (16)$$

1) After the replacement, $\nu_1, \nu_2, \nu_3, \nu_s$ are slightly changed and constitute the real mass eigenstate.

It is obvious that the multiplication $R_{23}R_{13}R_{12} \equiv U^0$ is the usual Pontecorvo [19]-Maki-Nakawaga-Sakata [20] (PMNS) matrix modified by adding a trivial fourth column and row.

In order not to contradict with the available experimental measurements of three-neutrino oscillations and the data of LEP, the mixing between sterile and active neutrinos must be very small. And here an assumption is made that the added sterile neutrino does not distinguish between the three active ones, i.e., the mixing angles $\theta_{34} = \theta_{24} = \theta_{14} \equiv \epsilon_1$. In Eq. (14) only squared mixing elements $|U_{\alpha i}|^2$ appear in $\Delta r_{P\alpha\beta}$ while neglecting

higher order powers of ϵ_1 , one obtains

$$\begin{aligned} |U_{\alpha i}|^2 &= |U_{\alpha i}^0|^2 \cos^2 \epsilon_1, (\alpha=e, \mu, \tau; i=1, 2, 3); \\ |U_{e4}|^2 &= \sin^2 \epsilon_1; |U_{\mu 4}|^2 = \sin^2 \epsilon_1 \cos^2 \epsilon_1; \\ |U_{\tau 4}|^2 &= \sin^2 \epsilon_1 \cos^4 \epsilon_1, \end{aligned} \quad (17)$$

where we ignore the subscript “3+1” in U_{3+1} and the $U_{\alpha i}^0$ refers to the elements of the unitary U^0 (3+0) with $\sum_{i=1}^3 |U_{\alpha i}^0|^2 = 1$ for $\alpha=e, \mu, \tau$.

Then with these mixing matrix elements, one can obtain $R_{P\alpha\beta}^s$ in the 3+1 scenario

$$R_{P\alpha\beta}^s = \frac{\cos^2 \epsilon_1 m_\alpha^2 (m_P^2 - m_\alpha^2)^2 + |U_{\alpha 4}|^2 (m_\alpha^2 + m_{s1}^2) (m_P^2 - m_\alpha^2 - m_{s1}^2) \lambda(m_P^2, m_\alpha^2, m_{s1}^2)}{\cos^2 \epsilon_1 m_\beta^2 (m_P^2 - m_\beta^2)^2 + |U_{\beta 4}|^2 (m_\beta^2 + m_{s1}^2) (m_P^2 - m_\beta^2 - m_{s1}^2) \lambda(m_P^2, m_\beta^2, m_{s1}^2)}, \quad (18)$$

which is substituted into Eq. (13) to obtain $\Delta r_{P\alpha\beta}$ under the 3+1 scenario.

3.2 3+2 scenario

Turning to the 3+2 scenario in which two sterile neutrinos are introduced, the procedure is similar to that for the 3+1 case. The mixing angles between the second sterile neutrino and active neutrinos are denoted as ϵ_2 . Then we summarize the results below:

$$\begin{aligned} |U_{\alpha i}|^2 &\approx |U_{\alpha i}^0|^2 \cos^2 \epsilon_1 \cos^2 \epsilon_2, (\alpha=e, \mu, \tau; i=1, 2, 3); \\ |U_{e4}|^2 &= \sin^2 \epsilon_1 \cos^2 \epsilon_2; |U_{e5}|^2 = \sin^2 \epsilon_2; \\ |U_{\mu 4}|^2 &= \sin^2 \epsilon_1 \cos^2 \epsilon_1 \cos^2 \epsilon_2; |U_{\mu 5}|^2 = \sin^2 \epsilon_2 \cos^2 \epsilon_2; \\ |U_{\tau 4}|^2 &\approx \sin^2 \epsilon_1 \cos^4 \epsilon_1 \cos^2 \epsilon_2; |U_{\tau 5}|^2 = \sin^2 \epsilon_2 \cos^4 \epsilon_2. \end{aligned} \quad (19)$$

With these elements one can obtain $\Delta r_{P\alpha\beta}$ with the 3+2 scenario.

3.3 Constraints set by the FCNC

With the scenarios discussed above, the neutrino neutral current (NC) interaction will be modified. As discussed above, the number of neutrinos is 2.984 ± 0.008 by fits to LEP data. Assuming that the small deviation from 3 is caused by mixing between active and sterile neutrinos, this value will cast rigorous constraints on the mixing parameter $\epsilon_{1,2}$. An estimate is: $\epsilon_1 \leq \mathcal{O}(5 \times 10^{-2})$ for the 3+1 scenario and $\epsilon_1^2 + \epsilon_2^2 \leq \mathcal{O}(10^{-3})$ for the 3+2 case. A preliminary result about sum $\sum_{i=1}^3 |U_{ei}| = 0.994 \pm 0.005$ at 90% confidence level [21], which signifies the non-unitarity of the 3×3 active neutrino mixing matrix to be at level $\leq \mathcal{O}(10^{-2})$ [22]. The non-vanishing terms $U_{\alpha\beta} \equiv \sum_{i=4}^N U_{\alpha i}^* U_{i\beta}$ ($\alpha \neq \beta$) result in the tree level FCNC interaction, which can induce the low-energy lepton flavor

violation (LFV) processes. These LFV processes are proportional to the value of the non-vanishing $\sum_{i=4}^N U_{\alpha i}^* U_{i\beta}$. The experimental bounds on these LFV interactions can be transformed to constraints on the new mixing angles $\epsilon_{1,2}$. For instance, constraints to $|U_{\alpha\beta}|$ from several LFV processes Ref. [23, 24]:

$$\begin{aligned} |U_{\mu e}| &< 3.05 \times 10^{-6} (\mathcal{B}(\mu^- \rightarrow e^- e^+ e^-) < 1.0 \times 10^{-12}), \\ |U_{\tau e}| &< 1.37 \times 10^{-3} (\mathcal{B}(\tau^- \rightarrow e^- e^+ e^-) < 3.6 \times 10^{-8}), \\ |U_{\tau \mu}| &< 1.295 \times 10^{-3} (\mathcal{B}(\tau^- \rightarrow \mu^- \mu^+ \mu^-) < 3.2 \times 10^{-8}). \end{aligned}$$

Considering these bounds and the elements derived above, with reasonable approximations we can obtain constraints on $\epsilon_{1,2}$ which are shown in Table 1.

4 Numerical analyses

In this section we numerically evaluate the total contributions from the SM and new physics BSM to $\Delta r_{P\alpha\beta}$ in the context of 3+1 and 3+2 scenarios to account for the observed data. The analyses are about the leptonic decays of pseudo-scalar mesons $P=\pi, K, D, D_s, B, B_c$. The evaluated branching ratios of the leptonic decays are listed in Table 2 and the corresponding $R_{P\alpha\beta}$ and $\Delta r_{P\alpha\beta}$ are shown in Table 3.

4.1 3+1 scenario

In this subsection, we make a numerical analysis on the breaking of the lepton universality in different decay processes, within the 3+1 scenario. $\Delta r_{\tau e\mu}$ and $\Delta r_{K e\mu}$ in the parameter space of mixing parameter ϵ_1 and sterile neutrino mass m_{s1} are shown in Fig. 1. The central value of $\Delta r_{P e\mu}$ is denoted by the solid line while its $1-\sigma$ region is enclosed by the dashed lines. In the left panel of Fig. 1 for $\Delta r_{\tau e\mu}$, to accommodate the experimental results,

Table 1. Constraints to new added mixing parameters $\epsilon_{1,2}$ from the experimental limits of LFV processes.

scenario	$ U_{\mu e} $	$ U_{\tau e} $	$ U_{\tau \mu} $
3+1	$\epsilon_1 < 1.75 \times 10^{-3}$	$\epsilon_1 < 3.70 \times 10^{-2}$	$\epsilon_1 < 3.599 \times 10^{-2}$
3+2	$\epsilon_1^2 + \epsilon_2^2 < 3.05 \times 10^{-6}$	$\epsilon_1^2 + \epsilon_2^2 < 1.37 \times 10^{-3}$	$\epsilon_1^2 + \epsilon_2^2 < 1.295 \times 10^{-3}$

Table 2. The experimental values or bounds of masses and branching ratios for $P=\pi, K, D, D_s, B, B_c$ taken from PDG [23]. The corresponding theoretical predictions are in (double) square brackets which are from Ref. ([25] [26]).

P	mass/MeV	$\mathcal{B}(P \rightarrow e\nu_e)$	$\mathcal{B}(P \rightarrow \mu\nu_\mu)$	$\mathcal{B}(P \rightarrow \tau\nu_\tau)$
π	139.57018 ± 0.00035	$(1.230 \pm 0.004) \times 10^{-4}$	$(99.98770 \pm 0.00004)\%$	—
K	(493.677 ± 0.016)	$(1.581 \pm 0.008) \times 10^{-5}$	$(63.55 \pm 0.11)\%$	—
D	(1869.62 ± 0.15)	$< 8.8 \times 10^{-6}$	$(3.82 \pm 0.33) \times 10^{-4}$	$< 1.2 \times 10^{-3}$
D_s	1968.49 ± 0.32	$< 1.2 \times 10^{-4}$	$[(4.15^{+0.22}_{-0.21}) \times 10^{-4}]$ $(5.90 \pm 0.33) \times 10^{-3}$	$[(1.10 \pm 0.06) \times 10^{-3}]$ $(5.43 \pm 0.31)\%$
B	5279.25 ± 0.17	$< 9.8 \times 10^{-7}$	$[(5.50^{+0.55}_{-0.52}) \times 10^{-3}]$ $< 1.0 \times 10^{-6}$	$[(5.36^{+0.54}_{-0.50}) \times 10^{-2}]$ $(1.65 \pm 0.34) \times 10^{-4}$
B_c	6277 ± 6	$[[(1.1 \pm 0.2) \times 10^{-11}]]$	$[[(4.5 \pm 1.0) \times 10^{-7}]]$	$[[(1.0 \pm 0.2) \times 10^{-4}]]$

Table 3. The current experimental measurements and SM prediction of $R_{P_{e\mu}}$ [26], $R_{P_{\mu\tau}}$ and the corresponding $\Delta r_{P_{\alpha\beta}}$. The SM predictions include the uncertainties from electromagnetic corrections and as well as the uncertainties due to CKM mixing matrix elements and decay constants.

P	$R_{P_{e\mu}}^{\text{exp}}$	$R_{P_{e\mu}}^{\text{SM}}$	$\Delta r_{P_{e\mu}}$
π	$(1.230 \pm 0.004) \times 10^{-4}$	1.234×10^{-4}	$(-3.241 \pm 3.241) \times 10^{-3}$
K	$(2.488 \pm 0.013) \times 10^{-5}$	$(2.472 \pm 0.001) \times 10^{-5}$	$(6.472^{+5.668}_{-5.664}) \times 10^{-3}$
P	$R_{P_{\mu\tau}}^{\text{exp}}$	$R_{P_{\mu\tau}}^{\text{SM}}$	$\Delta r_{P_{\mu\tau}}$
D	> 0.291	$0.377^{+0.043}_{-0.038}$	> -0.308
D_s	$0.109^{+0.013}_{-0.012}$	$(8.65^{+1.68}_{-1.43}) \times 10^{-2}$	$0.256^{+0.430}_{-0.317}$
B	$< 7.6 \times 10^{-3}$	$(4.5^{+2.4}_{-1.6}) \times 10^{-3}$	< 1.6
B_c	—	$(4.18^{+0.03}_{-0.04}) \times 10^{-3}$	—

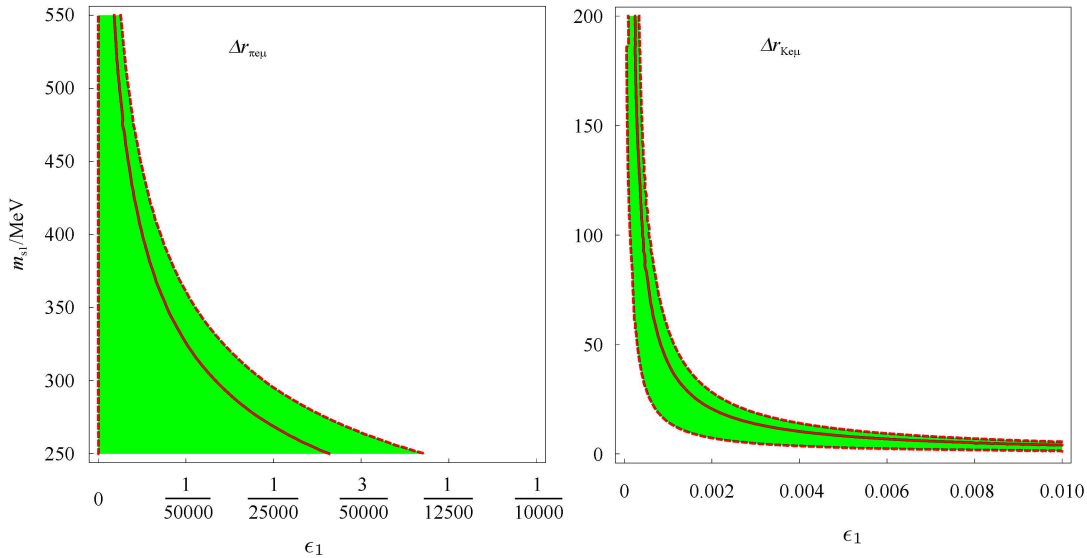


Fig. 1. The allowed parameter space of ϵ_1 and m_{s1} for $\Delta r_{\pi e\mu}$ and $\Delta r_{K e\mu}$.

the mass of the sterile neutrino has to be larger than 250 MeV, thus the final state with ν_s is kinematically forbidden. For $\Delta r_{Ke\mu}$, the allowed parameter space of ϵ_1 and m_{s1} is larger, which covers 0–400 MeV and 0–0.35, respectively. Also, in the region of $m_{s1} > m_K$, ν_s does not show up in the final state and the region with relatively larger ϵ_1 needs to be ruled out for its failure to be reconciled with the LEP data constraint.

Besides, as shown in Fig. 2, the 3+1 scenario fails to provide a common parameter space of ϵ_1 and m_{s1} to saturate the experimentally measured $\Delta r_{\pi e\mu}$ and $\Delta r_{Ke\mu}$ simultaneously, namely there does not exist a solution within 1σ tolerance.

Since both D_s to $\mu\nu$ and $\tau\nu$ have been experimentally measured, thus $\Delta r_{D_s\mu\tau}$ is obtained. A lack of experimental data on the decay rates of leptonic decays of D means that we cannot determine $\Delta r_{D\mu\tau}$ yet, for an illustration, we set the $\Delta r_{D\mu\tau}$ as $10^{-1}, 10^{-2}, 10^{-3}, 10^{-4}, 10^{-5}$ to get a sense of the dependence of the Δrs on ϵ_1 and m_{s1} . The results are shown in Fig. 3.

Form the figures of $\Delta r_{De\mu}$, $\Delta r_{D_s e\mu}$ and $\Delta r_{D\mu\tau}$ in

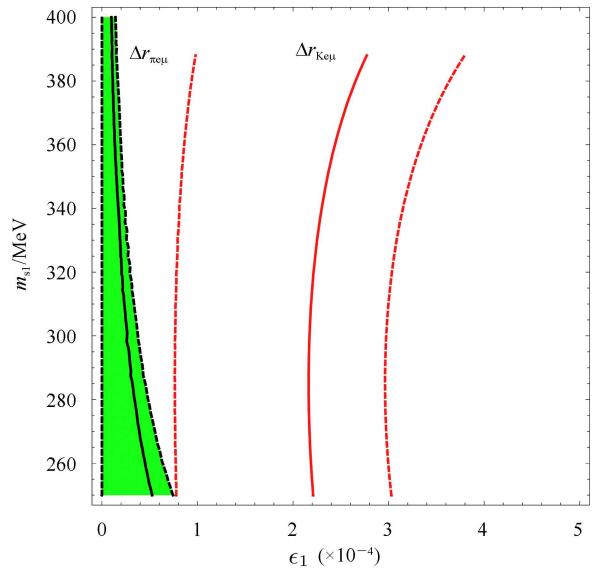


Fig. 2. Comparison of $\Delta r_{\pi e\mu}$ and $\Delta r_{Ke\mu}$ in the parameter spaces of mixing angles ϵ_1 and the sterile neutrino mass m_{s1} .

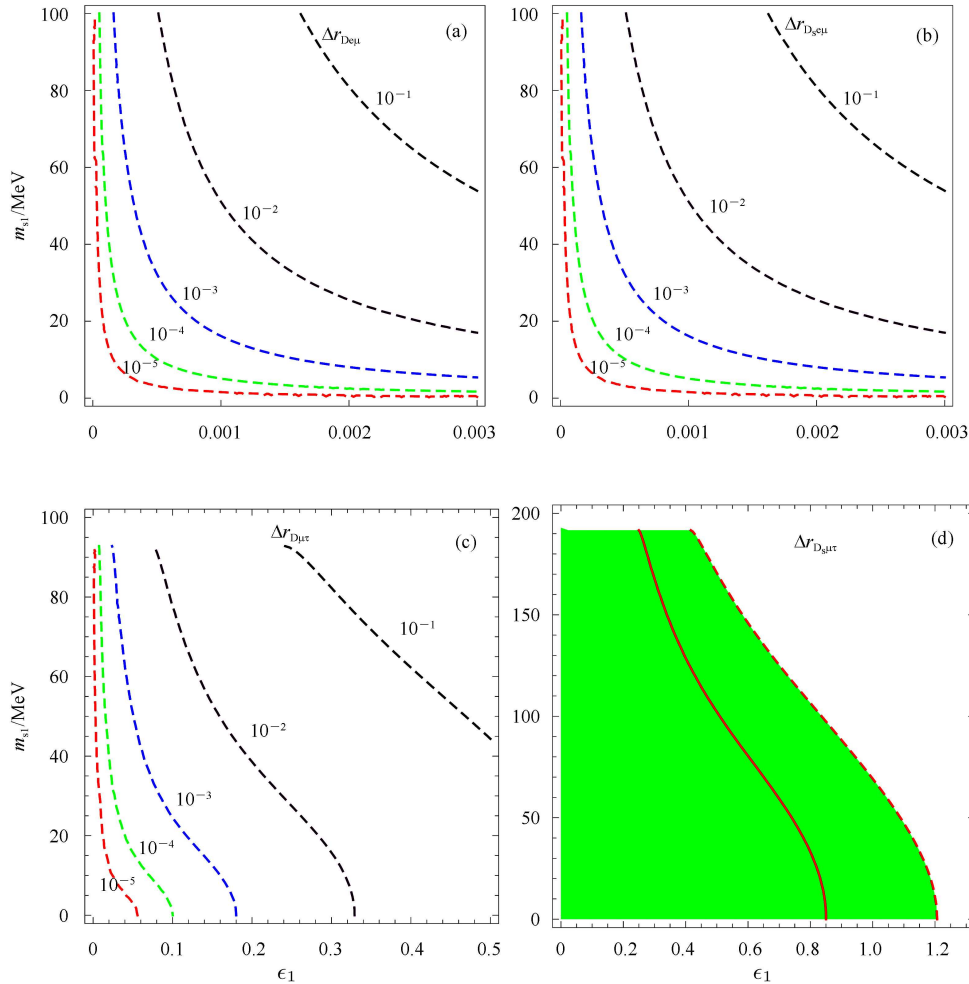


Fig. 3. $\Delta r_{De\mu}$, $\Delta r_{D_s e\mu}$, $\Delta r_{D\mu\tau}$, $\Delta r_{D_s\mu\tau}$ vs ϵ_1 and m_{s1} .

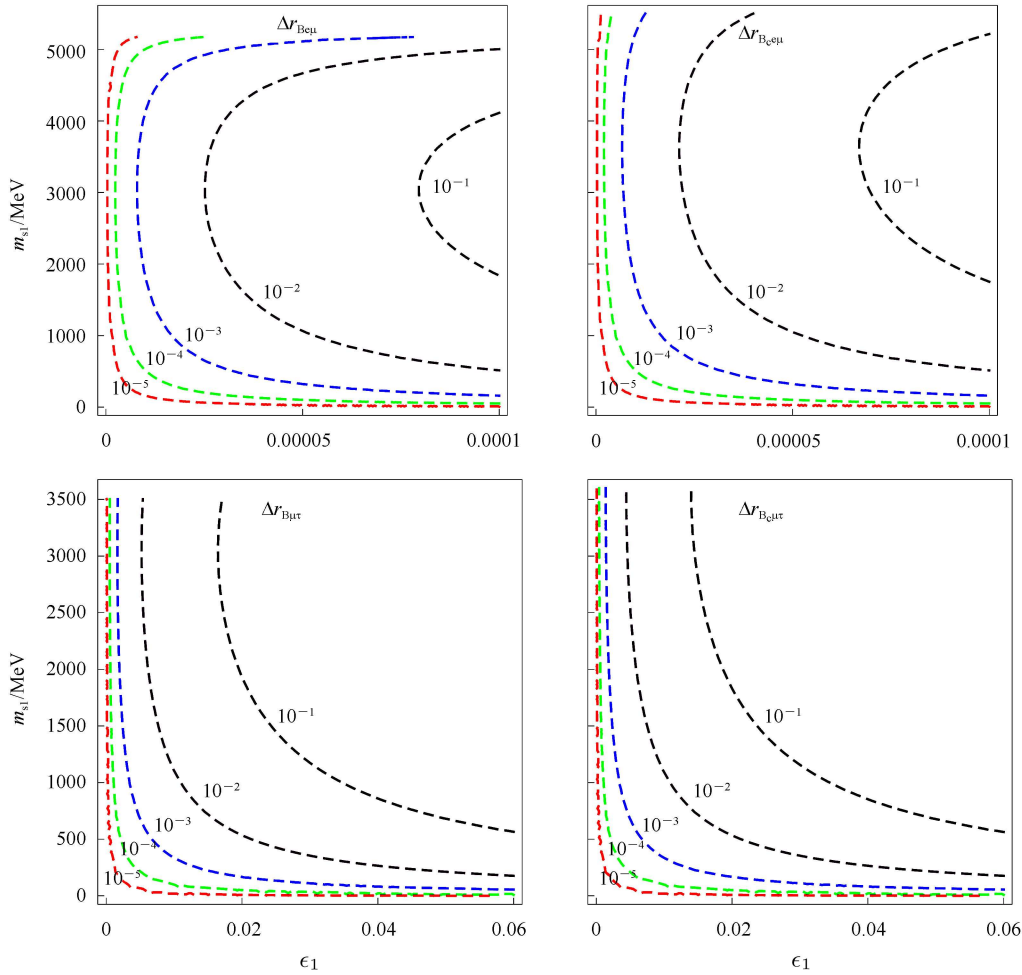

 Fig. 4. $\Delta r_{B_{ce\mu}}$, $\Delta r_{B_{c\mu\tau}}$, $\Delta r_{B_{\mu\tau}}$, $\Delta r_{B_{c\mu\tau}}$ vs ϵ_1 and m_{s1} .

Fig. 3, it is obvious that non-zero Δr demands non-vanishing ϵ_1 . Moreover, it is noted that for fixed m_{s1} (ϵ_1), the smaller Δr is, the smaller ϵ_1 (m_{s1}) would be.

In (d) of Fig. 3, the lower bound of $\Delta r_{D_s\mu\tau} = 0.256^{+0.430}_{-0.317}$ does not appear, as our analyses indicate that $\Delta r_{D_s\mu\tau}$ cannot be negative in the 3+1 scenario. From this diagram, it is obvious that within the $1-\sigma$ range of $\Delta r_{D_s\mu\tau}$, the particular values $\epsilon_1=0$ and ($m_{s1}=0$) are not excluded and the vanishing sterile-active neutrino mixing signifies that the lepton flavor universality holds. Thus to make a decisive judgement more accurate measurements are needed.

When discussing leptonic decays of B and B_c mesons, because of lack of experimental data, we take several values for Δr to illustrate its dependence on the parameters as shown in Fig. 4.

4.2 3+2 scenario

In this subsection, we numerically analyze the lepton universality with two sterile neutrinos, i.e., the 3+2

scenario.

Even though the errors are still large, $\Delta r_{\pi(K)e\mu}$ have been set, thus we first present $\Delta r_{\pi e\mu}$ and $\Delta r_{Ke\mu}$ in the same graph in Fig. 5, where the horizontal solid line corresponds to the central value and dashed lines enclose the $1-\sigma$ range of $\Delta r_{Ke\mu}$ whereas the perpendicular ones are for $\Delta r_{\pi e\mu}$.

The cross region satisfies both $\Delta r_{\pi e\mu}$ and $\Delta r_{Ke\mu}$. In our analyses, we let the mixing angles ϵ_1 and ϵ_2 vary within $(0, 3 \times 10^{-3})$ and $(0, 5 \times 10^{-5})$, respectively, while the sterile neutrino masses $m_{s1} \in (0, 140)$ MeV and $m_{s2} \in (0, 500)$ MeV. It is noted that for such parameter ranges, there exist solutions to accommodate both $\Delta r_{\pi e\mu}$ and $\Delta r_{Ke\mu}$. Concretely, the red points which correspond to the values calculated within the parameter ranges fall in the common region of these two quantities. Existence of solutions satisfying both $\Delta r_{\pi e\mu}$ and $\Delta r_{Ke\mu}$ signifies the success of the 3+2 model in explaining the observed lepton universality violation in π and K decays. Now we turn to D_s decays, whose rates have been

experimentally measured, but not yet sufficiently accurate, to see if we are able to determine $\Delta r_{D_s\mu\tau}$.

$\Delta r_{Ke\mu}$ and $\Delta r_{D_s\mu\tau}$ are presented in Fig. 6 where one notices that within the parameter ranges: $\epsilon_1 \in (0, 6 \times 10^{-4})$, $\epsilon_2 \in (0, 5 \times 10^{-5})$, $m_{s1} \in (1, 140)$ MeV, and $m_{s2} \in (0, 500)$ MeV, both $\Delta r_{Ke\mu}$ and $\Delta r_{D_s\mu\tau}$ can be satisfied. Especially, in these parameter ranges $\Delta r_{\pi e\mu}$ and $\Delta r_{Ke\mu}$ are also satisfied.

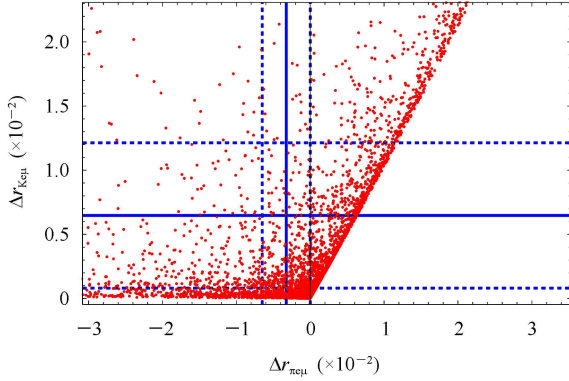


Fig. 5. The common solution for $\Delta r_{\pi e\mu}$ and $\Delta r_{Ke\mu}$ in the 3+2 scenario.

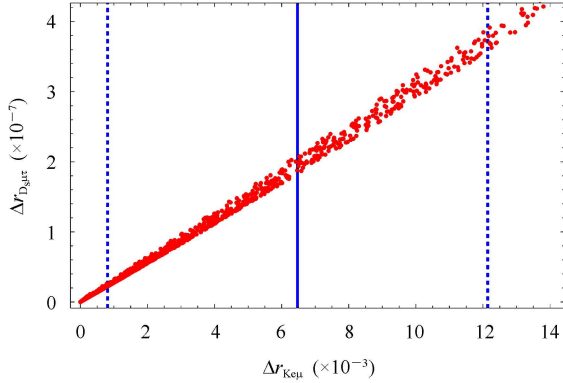


Fig. 6. The common solutions of $\Delta r_{Ke\mu}$ and $\Delta r_{D_s\mu\tau}$ in 3+2 scenario.

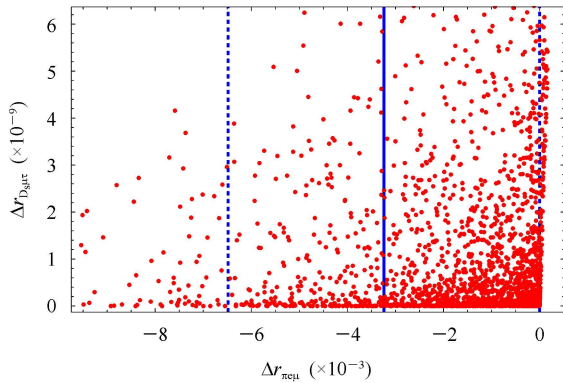


Fig. 7. The common region of $\Delta r_{\pi e\mu}$ and $\Delta r_{D_s\mu\tau}$ in 3+2 scenario.

The common region for $\Delta r_{\pi e\mu}$ and $\Delta r_{D_s\mu\tau}$ is shown in Fig. 7.

The similar analyses have been carried out for D, B, and B_c mesons. Due to shortage of data to calculate corresponding Δr s, we adopt the parameter ranges obtained by fitting $\Delta r_{\pi e\mu}$, $\Delta r_{Ke\mu}$ and $\Delta r_{D_s\mu\tau}$, to the leptonic decays of D, B and B_c and investigate if there exists a common region for $\Delta r_{Pe\mu} - \Delta r_{P\mu\tau}$ ($P=D, B, \text{ or } B_c$). The results are shown in Fig. 8 and Fig. 9.

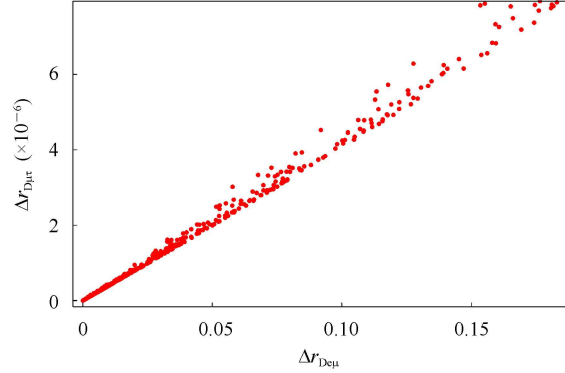


Fig. 8. The common solutions of $\Delta r_{De\mu}$ and $\Delta r_{D\mu\tau}$ in 3+2 scenario.

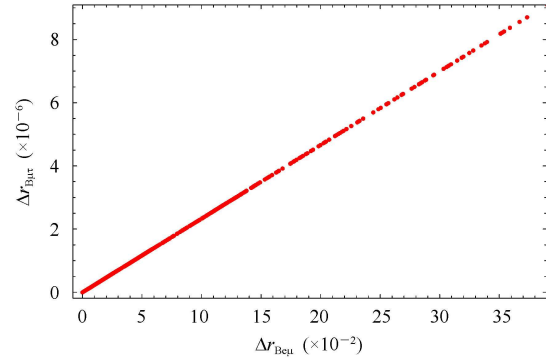


Fig. 9. The estimate of $\Delta r_{Be\mu}$ and $\Delta r_{B\mu\tau}$ in 3+2 scenario.

5 Testing LFU at BESIII

Experimental measurements of pure leptonic decays of D and D_s mesons have been carried out by many collaborations: via e^+e^- annihilation at Z^0 mass pole [27–29], at $\Upsilon(4S)$ mass [30, 31], and at $\sqrt{s}=3.773, 4.040$ or 4.170 GeV [32, 33], respectively. To test violation of the lepton flavor universality, very high accuracy is necessary. However, most of the the aforementioned experiments suffered from high background contamination, so do not meet the high accuracy demand. In this aspect, the electron-positron colliders prevail over others. Because charmed mesons are produced in pairs, one can

accurately measure the pure leptonic decays based on the double tag method.

For example, the e^+e^- annihilation experiment around the 3.773 GeV, which is just above the $D\bar{D}$ production threshold, a charmed meson and its anti-particle are produced in pairs, i.e., $\psi(3770) \rightarrow D\bar{D}$. If one fully identifies \bar{D} in one event, which is called a singly tagged \bar{D} meson, there must exist a D meson in the recoiling side against the tagged \bar{D} meson. If one reconstructs the whole $D\bar{D}$ pair in the analysis, the event will be called a double tag event. Thus, in an event which consists of a singly tagged D^- , the pure-leptonic modes can be selected from the final states of D^+ decays, and the absolute branching fractions would be well determined.

For the measurements around 4.040 or 4.170 GeV, situations are not much different except $D\bar{D}$ being replaced by $D_S^+D_S^-$ or $D_S^-D_S^{*+} + c.c.$

In the BESIII experiments, charmed mesons are collected at 3.773 and 4.040 GeV, respectively. Here we present a Monte Carlo (MC) simulation at these two energy points to discuss the experimental sensitivities of searching for pure-leptonic decays that can be reached in the future.

The MC events are generated with the BESIII offline software system [34], where the particle trajectories are simulated with the GEANT4 [35] based package [36] for the BESIII detector [37] at the BEPC-II collider.

The events used in this discussion are generated as $e^+e^- \rightarrow \psi(3770) \rightarrow D\bar{D}$ and $e^+e^- \rightarrow \psi(4040) \rightarrow D_S^+D_S^-$ at the c.m. energy $\sqrt{s} = 3.773$ and 4.040 GeV, respectively, where the $D\bar{D}$ and $D_S^+D_S^-$ mesons are set to decay into all possible final states with the branching fractions cited by PDG [23].

In total, $\sim 1.23 \times 10^8$ $D\bar{D}$ and $\sim 6.20 \times 10^6$ $D_S^+D_S^-$ events are generated at $\sqrt{s} = 3.773$ and 4.040 GeV, respectively, corresponding to an integrated luminosity of $\sim 20 \text{ fb}^{-1}$ $\psi(3770)$ and $\psi(4040)$ data assuming $\sigma_{DD}^{\text{obs}} = 6.14 \text{ nb}$ [38] and $\sigma_{D_S^+D_S^-}^{\text{obs}} = 0.31 \text{ nb}$ [39], which contains $\sim 7.2 \times 10^7$ $D^0\bar{D}^0$ pairs, $\sim 5.1 \times 10^7$ D^+D^- pairs and 6.20×10^6 $D_S^+D_S^-$ pairs respectively. The BEPC-II collider is designed to work with an instantaneous luminosity of $10^{33} \text{ cm}^{-2}\text{s}^{-1}$ around $\psi(3770)$. As a conservative estimate, a data sample with an integrated luminosity of about 20 fb^{-1} can be collected during more than 10 years' running.

The singly tagged D^- and D_S^- events are reconstructed in 9 hadronic decays of $D^- \rightarrow K^+\pi^-\pi^-$ (50%), $D^- \rightarrow K_S^0\pi^-$ (52%), $D^- \rightarrow K_S^0K^-$ (48%), $D^- \rightarrow K^+K^-\pi^-$ (40%), $D^- \rightarrow K^+\pi^-\pi^-\pi^0$ (28%), $D^- \rightarrow \pi^+\pi^-\pi^-$ (56%), $D^- \rightarrow K_S^0\pi^-\pi^0$ (27%), $D^- \rightarrow K^+\pi^+\pi^-\pi^-\pi^-$ (21%), $D^- \rightarrow K_S^0\pi^-\pi^-\pi^+$ (31%) and 9 hadronic decays of $D_S^- \rightarrow K_S^0K^-$ (46%), $D_S^- \rightarrow K^+K^-\pi^-$ (39%), $D_S^- \rightarrow K^+K^-\pi^-\pi^0$ (12%), $D_S^- \rightarrow K_S^0K^+\pi^-\pi^-$ (24%), $D_S^- \rightarrow \pi^-\pi^+\pi^-$ (52%), $D_S^- \rightarrow \pi^-\eta$, $\eta \rightarrow \gamma\gamma$ (41%), $D_S^- \rightarrow \pi^-\eta'$, $\eta' \rightarrow \pi^+\pi^-\eta$, $\eta \rightarrow \gamma\gamma$

(21%), $D_S^- \rightarrow \pi^-\eta'$, $\eta' \rightarrow \gamma\rho^0$ (34%), $D_S^- \rightarrow \rho^-\eta$ (17%) constituting approximately 29% of all D^- decays and 30% D_S^- decays, respectively, where the numbers in brackets are reconstruction efficiencies.

Tagged D^- and D_S^- events are selected by two kinematic variables based on the principles of energy and momentum conservations: (1) difference in energy

$$\Delta E \equiv E_f - E_b, \quad (20)$$

where E_f is the total energy of the daughter particle from D^- or D_S^- in one event and E_b is the e^+/e^- beam energy for the experiment, is recorded to describe the deviation from energy conservation caused by experimental errors.

(2) Beam-constrained mass

$$M_{\text{BC}} \equiv \sqrt{E_b^2 - (\sum_i \vec{p}_i)^2} \quad (21)$$

is calculated to reduce an uncertainty caused by experimental errors when measuring the momenta of the produced particles. By this definition, the energy E_f in the expression of

$$M_{\text{inv.}}^2 \equiv E_f^2 - p_f^2$$

for the \bar{D} invariant mass is replaced by $E_b = E_{\text{c.m.}}/2$, where $E_{\text{c.m.}}$ is the c.m. energy at which D^+D^- pair is produced.

The total energy and momentum of all the daughter particles in D^\pm and D_S decays must satisfy the energy conservation (EC) principle, generally one needs to introduce a kinematic fit, including energy and momentum constraints and some relevant corrections, to reject those not satisfying EC, but being recorded due to an uncertainty of experimental measurement. This replacement of the real invariant mass by M_{BC} partly plays the role.

Moreover, events are rejected if they fail to satisfy the selection constraint $|\Delta E| < 3 \times \sigma_{\Delta E}$, which is tailored for each individual decay mode, and $\sigma_{\Delta E}$ is the standard deviation of the ΔE distribution.

As the D^\pm and D_S events are correctly tagged, a peak in the M_{BC} spectrum would emerge at the position of D^- or D_S^- mass. Finally, if there are more than one combinations in one tagged event, the one with the smallest $|\Delta E|$ is retained. After considering the detection efficiencies of each tag mode, 10837045 ± 6122 and 549811 ± 1593 tagged D^- and \bar{D}_S events are obtained based on data samples of about 20 fb^{-1} , respectively.

At the recoiling side against the tagged meson, the other charmed meson decays into a charged lepton and a neutrino. Since the neutrino does not electromagnetically interact with detector matter, it cannot be recorded in the detector and contributes a missing energy, therefore, a kinematic quantity is defined

$$M_{\text{miss}}^2 \equiv (E_b - E_{l^+})^2 - (-\vec{p}_{D^-/D_S^-} - \vec{p}_{l^+})^2, \quad (22)$$

where \vec{p}_{D^-/D_S^-} is the three-momentum of the fully reconstructed D^-/D_S^- , and E_{l^+} (\vec{p}_{l^+}) is the energy (momentum) of the candidate lepton. The spectrum of M_{miss}^2 for the signal events should produce a peak near zero because the neutrino mass is very tiny.

To select the purely leptonic decay event of $D^+ \rightarrow l^+ \nu_l$, only one charged track identified as electron/muon/pion and no isolated photons are allowed at the recoiling side.

For the rare process of $D^+ \rightarrow e^+ \nu_e$, the signal number is determined to be 1 by counting the signal window of M_{miss}^2 . We set an upper limit on the number of signal events for $D^+ \rightarrow e^+ \nu_e$ to be 4.36 by using the Feldman-Cousins method [40] in the absence of background at 90% confidence level. The upper limit on the branching fraction for $D^+ \rightarrow e^+ \nu_e$ is $\mathcal{B}(D^+ \rightarrow e^+ \nu_e) < 8.5 \times 10^{-7}$.

For the decay of $D^+ \rightarrow \mu^+ \nu_\mu$, the number of simulated signal events is obtained to be $N_{D^+ \rightarrow \mu^+ \nu_\mu}^{\text{obs}} = 2611.1 \pm 55.0$ by fitting the M_{miss}^2 distribution, and the efficiency for reconstructing $D^+ \rightarrow \mu^+ \nu_\mu$ against the tag side is estimated to be $N_{D^+ \rightarrow \mu^+ \nu_\mu}^{\text{obs}} = (63.82 \pm 0.15)\%$. Therefore, the branching fraction for $D^+ \rightarrow \mu^+ \nu_\mu$ is calculated to be $\mathcal{B}(D^+ \rightarrow \mu^+ \nu_\mu) = (3.74 \pm 0.08(\text{stat.})) \times 10^{-4}$.

For $D^+ \rightarrow \tau^+ \nu_\tau$, with $\tau^+ \rightarrow \pi^+ \bar{\nu}_\tau$, the missing mass squared M_{miss}^2 for the candidate events is calculated as

$$M_{\text{miss}}^2 \equiv (E_b - E_{\pi^+})^2 - (-\vec{p}_{D^+} - \vec{p}_{\pi^+})^2. \quad (23)$$

Since there are two missing neutrinos, the M_{miss}^2 does not have a narrow peak as in the decay of $D^+ \rightarrow \mu^+ \nu_\mu$. To suppress the background from $D^+ \rightarrow K_L^0 \pi^+$ by missing K_L^0 and $D^+ \rightarrow \mu^+ \nu_\mu$ by μ/π mis-identification, the M_{miss}^2 is studied in two cases defined by $E_\pi^{\text{EMC}} > 0.3$ and $E_\pi^{\text{EMC}} < 0.3$ GeV, resulting the number of signal events for $D^+ \rightarrow \tau^+ \nu_\tau$ to be 312.1 ± 28.2 and 242.9 ± 26.1 , respectively. With these signal events, inputting the detection efficiency of $(17.16 \pm 0.14)\%$ and $(13.33 \pm 0.12)\%$, the branching fraction is determined to be $\mathcal{B}(D^+ \rightarrow \tau^+ \nu_\tau) = (1.68 \pm 0.12(\text{stat.})) \times 10^{-3}$, which is averaged by $(1.68 \pm 0.16(\text{stat.})) \times 10^{-3}$ and $(1.68 \pm 0.18(\text{stat.})) \times 10^{-3}$ for the two cases.

Following the similar analysis, the number of signal events for $D_S^+ \rightarrow l^+ \nu_l$ is determined to be $N_{D_S^+ \rightarrow e^+ \nu_e}^{\text{obs}} = 1$, $N_{D_S^+ \rightarrow \mu^+ \nu_\mu}^{\text{obs}} = 2335.5 \pm 55.1$ and $N_{D_S^+ \rightarrow \tau^+ \nu_\tau}^{\text{obs}} = 11484.1 \pm 110.2$, with the corresponding detection efficiencies to be $\epsilon_{D_S^+ \rightarrow e^+ \nu_e}^{\text{obs}} = (46.94 \pm 0.16)\%$, $\epsilon_{D_S^+ \rightarrow \mu^+ \nu_\mu}^{\text{obs}} = (70.41 \pm 0.14)\%$ and $\epsilon_{D_S^+ \rightarrow \tau^+ \nu_\tau}^{\text{obs}} = (39.41 \pm 0.16)\%$, respectively. Inserting the numbers of events and upper limit at 90% C.L. for $D_S^+ \rightarrow e^+ \nu_e$, the branching fractions are calculated to be $\mathcal{B}(D_S^+ \rightarrow e^+ \nu_e) < 1.69 \times 10^{-5}$, $\mathcal{B}(D_S^+ \rightarrow \mu^+ \nu_\mu) = (6.03 \pm 0.14(\text{stat.})) \times 10^{-3}$, and $\mathcal{B}(D_S^+ \rightarrow \tau^+ \nu_\tau) = (5.30 \pm 0.05(\text{stat.}))\%$.

Based on these simulation results, the ratio of decay rates to different leptons can be obtained to test the lep-

ton universality. With 20 fb⁻¹ BESIII data samples at c.m. energy of 3.773 and 4.040 GeV, the ratios are

$$R_{D_{e\mu}} = \frac{\Gamma(D^+ \rightarrow e^+ \nu_e)}{\Gamma(D^+ \rightarrow \mu^+ \nu_\mu)} < 2.26 \times 10^{-3}, \quad (24)$$

and

$$R_{D_{\mu\tau}} = \frac{\Gamma(D^+ \rightarrow \mu^+ \nu_\mu)}{\Gamma(D^+ \rightarrow \tau^+ \nu_\tau)} = 0.223 \pm 0.017(\text{stat.}) \quad (25)$$

for charm meson, and

$$R_{D_{Se\mu}} = \frac{\Gamma(D_S^+ \rightarrow e^+ \nu_e)}{\Gamma(D_S^+ \rightarrow \mu^+ \nu_\mu)} < 2.80 \times 10^{-3}, \quad (26)$$

$$R_{D_{S\mu\tau}} = \frac{\Gamma(D_S^+ \rightarrow \mu^+ \nu_\mu)}{\Gamma(D_S^+ \rightarrow \tau^+ \nu_\tau)} = 0.114 \pm 0.003(\text{stat.}) \quad (27)$$

for the strange-charmed meson. The experimental sensitivities for the above measurement with 10 years' (20 fb⁻¹) data accumulation are $\Delta_{R_{D^+ \mu\tau}} \sim 7.35\%$ and $\Delta_{R_{D_S^+ \mu\tau}} \sim 2.50\%$, however, the size of these huge data samples cannot present a solid estimate for the electron decays. The theoretical expectation for electron mode is at 10⁻⁵ level, to challenge this limit, there should be a desperate running time for the BESIII experiment. Fortunately, it will not be a problem if one can build a τ -charm factory with an increasing of the luminosity of about 100 times.

The luminosity of BEPC II is not high enough, so to fulfill the job, one needs at least 10 years of machine running. However as suggested, the planned charm-tau factory will greatly enhance the luminosity and with the new facility, we expect that in a few months a sufficiently large database could be collected and then one may have required accuracy to testify the lepton universality.

6 Discussions and conclusions

In this work we study the lepton universality in the 3+1 and 3+2 scenarios. The analyses indicate that by adding one sterile neutrino to the SM, i.e., the 3+1 scenario, the Δr s reflecting the differences between experimental data and SM predictions in the leptonic decays of various pseudoscalar mesons cannot be accommodated simultaneously for various mesons. Therefore, the 3+1 scenario is attractive for its simplicity, but does not meet the data. Whereas the 3+2 scenario has less tension in accordance with the data. However, although there still exists difficulty in choosing a proper mass range for the second sterile neutrino, the current experimental data on $\Delta r_{\pi e\mu}$, $\Delta r_{K e\mu}$, and $\Delta r_{D_S \mu\tau}$ can be well accommodated. This result motivates one to be inclined to involve more sterile neutrinos, i.e., the 3+3 model. With the param-

ter ranges selected by fitting the data for π , K and D_s , the predicted values of Δr s for D, B, and B_c are obtained which will be tested by future experiments such as the Z-factory and LHCb.

Usually it is believed that the μ - τ symmetry [41] holds at high-energy scales, but breaks during the evolution to low-energy, so that the 3×3 PMNS mixing matrix for active neutrinos deviates from the original symmetric textures. The violation of lepton universality, especially that for μ - τ universality, might be a low-energy behavior as the universality precisely holds at high-energy scale, say, the GUT or the see-saw energy scales. These assumptions motivate relating the breaking of the μ - τ symmetry to the violation of the μ - τ universality. The idea is that the symmetry breaking that leads to a real PMNS matrix and the LFU violation may originate from same source and be caused by the same mechanism. Thus both of them serve as the low-energy manifestations of the symmetry breaking.

In order to obtain a negative value for Δr , $R_{P\alpha\beta}^s$ should be smaller than the value predicted by the SM

$R_{P\alpha\beta}^{\text{SM}}$. Then one can obtain

$$R_{P\alpha\beta}^{\text{SM}} < \frac{\sum_{j=1}^{N-3} |U_{\beta,j+3}|^2 (m_\beta^2 + m_{sj}^2) (m_P^2 - m_\beta^2 - m_{sj}^2) \lambda(m_P^2, m_\beta^2, m_{sj}^2)}{\sum_{i=1}^{N-3} |U_{\alpha,i+3}|^2 (m_\alpha^2 + m_{si}^2) (m_P^2 - m_\alpha^2 - m_{si}^2) \lambda(m_P^2, m_\alpha^2, m_{si}^2)}, \quad (28)$$

i.e., the ratio of the contributions from sterile neutrino should be larger than the SM prediction $R_{P\alpha\beta}^{\text{SM}}$.

Obviously, ignoring high order QED radiative corrections, only the mass of the concerned pseudoscalar meson enters the game, but not the identities of its constituents, thus we can relate Δr s of various mesons to each others. This conclusion is viable for checking the scenarios discussed in the introduction.

The error tolerance still does not exclude the probability of $\Delta r=0$, then to check violation of LFU, a high-luminosity charm-tau factory and/or B-factory are necessary to draw a solid conclusion.

References

- 1 The LEP Collaborations, the LEP Electroweak Working Group, and the SLD Heavy Flavor and Electroweak Groups. CERN-EP/2003-091, arXiv: hep-ex/0312023
- 2 Filipuzzi A, Gonzalez-Alonso M, Portoles J. Phys. Rev. D, 2012, **85**: 116010
- 3 Abada A, Das D, Teixeira A M, Vicente A, Weiland C. arXiv: 1211.3052[hep-ph]
- 4 HOU Wei-Shu. Phys. Rev. D, 1993, **48**: 2342
- 5 Lopez-Val D, Sola J. arXiv:1211.0311 [hep-ph]
- 6 Masiero A, Paradisi P, Petronzio R. Phys. Rev. D, 2006, **74**: 011701; Masiero A, Paradisi P, Petronzio R. JHEP, 2008, **0811**: 042; Ellis J, Lola S, Raidal M, Nucl. Phys. B, 2009, **812**: 128; Girrbach J, Nierste U. arXiv:1202.4906 [hep-ph]; Fonseca R M, Romao J C, Teixeira A M. Eur. Phys. J. C, 2012, **72**: 2228
- 7 Minkowski P. Phys. Lett. B, 1977, **67**: 421; Yanagida T. In: Proc. of the Workshop on Unifed Theory and the Baryon Number of the Universe. Sawada O & Sugamoto A. Tsukuba: KEK, 1979. 95; Gell-Mann M, Ramond P, Slansky R. Supergravity. Amsterdam: North-Holland, 1979. 315; Glashow S L. Quarks and Leptons. New York: Plenum, 1980. 707; Mohapatra R N, Senjanovic G. Phys. Rev. Lett., 1980, **44**: 912
- 8 XING Zhi-Zhong, ZHOU Shun. Neutrinos in Particle Physics, Astronomy and Cosmology. Zhejiang University Press and Springer-Verlag, 2011
- 9 Wyler D, Wolfenstein L. Nucl. Phys. B, 1983, **218**: 205; Mohapatra R N, Valle J W F. Phys. Rev. D, 1986, **34**: 1642; Ma E. Phys. Lett. B, 1987, **191**: 287
- 10 Aguilar A et al. (LSND collaboration). Phys. Rev. D, 2001, **64**: 112007
- 11 Aguilar-Arevalo A A et al. (MiniBooNE collaboration). Phys. Rev. Lett., 2010, **105**: 181801
- 12 Mueller Th A et al. Phys. Rev. C, 2011, **83**: 054615
- 13 Anselmann P et al. (GALLEX collaboration.). Phys. Lett. B, 1995, **342**: 440; Hampel W et al. (GALLEX collaboration). Phys. Lett. B, 1998, **420**: 114; Kaether F et al. Phys. Lett. B, 2010, **685**: 47
- 14 Abdurashitov D et al. Phys. Rev. Lett., 1996, **77**: 4708; Abdurashitov J et al. (SAGE collaboration). Phys. Rev. C, 1999, **59**: 2246; Abdurashitov J et al. Phys. Rev. C, 2006, **73**: 045805; Abdurashitov J et al. (SAGE collaboration). Phys. Rev. C, 2009, **80**: 015807
- 15 ZHAO Gong-Bo et al. arXiv:1211.3741 [astro-ph.CO]
- 16 Goudzovski E. (NA48/2 and NA62 collaborations). arXiv:1111.2818 [hep-ex]
- 17 Balev S. arXiv:1006.1201 [hep-ex]
- 18 Abazajian K N et al. arXiv:1204.5379 [hep-ph]
- 19 Pontecorvo B. Zh. Eksp. Theor. Fiz., 1957, **33**: 549; Pontecorvo B. Zh. Eksp. Theor. Fiz., 1958, **34**: 247
- 20 Maki Z, Nakagawa M, Sakata S. Prog. Theor. Phys., 1962, **28**: 870
- 21 Antusch S et al. JHEP, 2006, **0610**: 084
- 22 XING Zhi-Zhong. arXiv: 1210.1523[hep-ph]
- 23 Beringer J et al. (Particle Data Group). Phys. Rev. D, 2012, **86**: 010001
- 24 Mohanta R. Eur. Phys. J. C, 2011, **71**: 1625
- 25 Aubert B et al. (The BABAR collaboration). arXiv: 0912.2453 [hep-ex]
- 26 Crivellin A, Kokulu A, Greub C. arXiv:1303.5877 [hep-ph]
- 27 Heister A et al. (ALEPH collaboration). Phys. Lett. B, 2002, **528**: 1
- 28 Abbiendi G et al. (OPAL collaboration). Phys. Lett. B, 2001, **516**: 236
- 29 Acciarri M et al. (L3 collaboration). Phys. Lett. B, 1997, **396**: 327
- 30 del Amo Sanchez P et al. (Babar collaboration). Phys. Rev. D, 2010, **82**: 091103
- 31 Widhalm L et al. (BELLE collaboration). Phys. Rev. Lett., 2008, **100**: 241801
- 32 Bonvicini G et al. (CLEO collaboration). Phys. Rev. D, 2004, **70**: 112004; Artuso M et al. (CLEO collaboration). Phys. Rev. Lett., 2005, **95**: 251801; Rubin P et al. (CLEO collaboration). Phys. Rev. D, 2006, **73**: 112005; Pedlar T K et al. (CLEO collaboration). Phys. Rev. D, 2007, **76**: 072002; Eisenstein B I et al. (CLEO collaboration). Phys. Rev. D, 2008, **78**: 052003; Ecklund K M et al. (CLEO collaboration). Phys. Rev. Lett., 2008, **100**: 161801; Alexander J P et al. (CLEO collaboration).

- Phys. Rev. D, 2009, **79**: 052001; Onyisi P U E et al. (CLEO collaboration). Phys. Rev. D, 2009, **79**: 052002; Naik P et al. (CLEO collaboration). Phys. Rev. D, 2009, **80**: 112004
- 33 BAI J Z et al. (BES collaboration). Phys. Rev. Lett., 1995, **74**: 4599; Bai J Z et al. (BES collaboration). Phys. Lett. B, 1998, **492**: 188; Ablikim M et al. (BESIII collaboration). Phys. Lett. B, 2005, **610**: 183
- 34 LI W D et al. The Offline Software for the BES Experiment. Proceeding of CHEP06. Mumbai, India 13-17 Febuary 2006
- 35 Agostinelli S et al. (Geant4 collaboration), Nucl. Instrum. Meth. A, 2003, **506**: 250
- 36 DENG Z Y et al. High Energy Phys. Nucl. Phys., 2003, **30**: 250
- 37 Ablikim M et al (BESIII collaboration). Nucl. Instrum. Methods A, 2010, **614**: 345
- 38 Ablikim M et al. (BES collaboration). Phys. Lett. B, 2004, **603**: 130
- 39 BAI J Z et al. (BES collaboration). Phys. Rev. D, 2000, **62**: 012002
- 40 Feldman G J, Cousins R D. Phys. Rev. D, 1998, **57**: 3873
- 41 Mohapatra R N, Smirnov A Yu. Ann. Rev. Nucl. Part. Sci., 2006, **56**: 569; GE Shao-Feng, HE Hong-Jian, YIN Fu-Rong. JCAP, 2010, **1005**: 017; HE Hong-Jian, YIN Fu-Rong. Phys. Rev. D, 2011, **84**: 033009; Adhikary B, Ghosal A, Roy P. arXiv:1210.5328 [hep-ph]